

OPEN ACCESS

EDITED BY Xiancan Zhu, Anhui Normal University, China

REVIEWED BY
Dao-Jun Guo,
Hexi University, China
Xiaoxu Li,
Beijing Life Science Academy, China

*CORRESPONDENCE
Gang Gu

☑ gugang318@163.com
Xiangmin Lin
☑ xiangmin@fafu.edu.cn
Xiaofang Xie
☑ xxf317@fafu.edu.cn

RECEIVED 30 May 2025 ACCEPTED 29 August 2025 PUBLISHED 15 September 2025

CITATION

Zhang B, Yang T, Cheng C, Li T, Zhang N, Wang F, Chen W, Zhong Z, Liu Z, Gu G, Lin X and Xie X (2025) Multi-omics analysis reveals the alleviating effect of oxidation remediation on tobacco quinclorac stress. *Front. Microbiol.* 16:1625585. doi: 10.3389/fmicb.2025.1625585

COPYRIGHT

© 2025 Zhang, Yang, Cheng, Li, Zhang, Wang, Chen, Zhong, Liu, Gu, Lin and Xie. This is an open-access article distributed under the terms of the Creative Commons Attribution License (CC BY). The use, distribution or reproduction in other forums is permitted, provided the original author(s) and the copyright owner(s) are credited and that the original publication in this journal is cited, in accordance with accepted academic practice. No use, distribution or reproduction is permitted which does not comply with these terms.

Multi-omics analysis reveals the alleviating effect of oxidation remediation on tobacco quinclorac stress

Binghui Zhang^{1,2}, Ting Yang¹, Chenliang Cheng³, Tong Li¹, Ni Zhang¹, Fei Wang³, Wencan Chen³, Zhiping Zhong⁴, Zhaoxiang Liu⁴, Gang Gu^{2*}, Xiangmin Lin^{1*} and Xiaofang Xie^{1,5*}

¹College of JunCao Science and Ecology, College of Life Sciences, Fujian Agriculture and Forestry University, Fuzhou, China, ²Institute of Tobacco Science, Fujian Provincial Tobacco Company, Fuzhou, China, ³Jianning Branch of Sanming Tobacco Company, Sanming, China, ⁴Changting Branch of Longyan Tobacco Company, Longyan, China, ⁵Fujian Key Laboratory of Crop Breeding by Design, Fujian Agriculture and Forestry University, Fuzhou, China

The extensive use of the herbicide quinclorac has led to significant residues in agricultural soil, posing adverse effects on crop safety and high-quality production. In this study, using the tobacco variety CB-1 as material, we found that oxidizing agent K₂S₂O₈ can significantly reduce quinclorac-induced phytotoxicity symptoms in tobacco. Furthermore, we integrated biochemical methods, metagenomics, metabolomics, and transcriptomics to investigate the effects of K₂S₂O₈ on both quinclorac-contaminated soil and tobacco plants. Soil physicochemical properties analysis showed that the incorporation of K₂S₂O₈-based remediation significantly mitigated the negative effects of quinclorac and largely restored the soil properties affected by quinclorac stress. Metagenomic analysis found that quinclorac significantly reduced soil species diversity, while K₂S₂O₈-based remediation soil exhibited higher richness of microbial communities, with increased abundance of Sphingomonas and Bradyrhizobium, and decreased abundance of Alphaproteobacteria. Differential gene expression analysis showed significant up-regulation and down-regulation of genes under C₁₀H₅Cl₂NO₂ stress, which was partially mitigated by $K_2S_2O_8$ treatment. Gene Ontology (GO) enrichment analysis indicated that these genes were mainly involved in cellular processes, metabolic pathways, and biological regulation. Metabolomic analysis further confirmed significant changes in metabolite profiles, with $K_2S_2O_8$ treatment restoring many metabolites to near control levels. Integrated metabolomic-transcriptomic analysis revealed enrichment of differentially expressed genes (DEGs) and metabolites in six key pathways: (1) lysine degradation, (2) stilbenoid diarylheptanoid and gingerol biosynthesis, (3) arginine and proline metabolism, (4) phenylalanine biosynthesis, (5) tyrosine metabolism, and (6) flavonoid biosynthesis. Additionally, the levels of 4-hydroxyphenylacetylglutamic and 5-aminovaleric acid were down-regulated, along with the expression of genes associated with these metabolites, when quinclorac residual soil was treated by K₂SO₈. The results of this study provide a theoretical basis for the remediation of pesticide residue soil in rice tobacco rotation areas, offering valuable insights for sustainable agricultural practices.

KEYWORDS

muti-omics, $K_2S_2O_8$, $C_{10}H_5C_2NO_2$, oxidation repair, tobacco

1 Introduction

Herbicides play an important role in reducing weed damage and promoting global food production security in current agricultural practices (Li et al., 2024). Among them, quinclorac with the molecular formula C₁₀H₅Cl₂NO₂ is a growth hormone-like herbicide known for its strong selectivity and long persistence, widely used to control monocotyledonous weeds in rice fields (Kieling and Pfenning, 1990). However, due to its relatively stable structure, quinclorac is difficult to degrade and prone to residue in acidic soils of southern regions, which may cause phytotoxicity on subsequent crops (Zang et al., 2020), especially on Solanaceous crops such as tobacco, potato, tomato, and eggplant (Qiuzan et al., 2018). In the rotation areas of tobacco-rice cultivation in southern China, quinclorac leads to leaf deformities (such as curling or narrowing) in tobacco plants, affecting both yield and quality of tobacco leaves and causing significant economic losses for farmers (Huang et al., 2021). Therefore, it is urgent to find solutions for alleviating the toxicity caused by quinclorac.

Soil remediation is considered the primary method for reducing the phytotoxicity of quinclorac on tobacco. The remediation process for land pollution can be categorized into two types: in situ and ex situ (Marcon et al., 2021). In situ remediation directly treats pollution sources without extra costs, making it the optimal choice. It encompasses three key strategies: bioremediation, physical remediation, and chemical oxidation remediation (Bains et al., 2019; He et al., 2015; Sun et al., 2017; Yu et al., 2019). Physical remediation has high costs and labor intensity. Additionally, when adsorbents reach the saturation point over time it leads to pesticide residues accumulating and losing their effectiveness (Dermont et al., 2008). In contrast, chemical oxidation remediation shows great potential in dealing with emerging pollutants. The oxidants used include ozone, Fenton reagent, potassium permanganate (KMnO4), and persulfate (Zeng et al., 2016). Among them, persulfate exhibits a higher redox potential resulting in longer lifespan during reactions with organic pollutants while facilitating better contact with pollutants (Yen et al., 2011). It has been successfully applied in degrading various pollutants such as PAHs (polycyclic aromatic hydrocarbons), PBDEs (polybrominated diphenyl ethers), PNP (p-nitrophenol), and atrazine (Chen et al., 2016, 2018; Peng et al., 2017; Song et al., 2019). To date, there have been no reports on the use of the oxidizing agent K₂S₂O₈ for the remediation of soil contaminated with quinclorac.

Non-biological stressors such as pesticides can simultaneously induce changes in crop rhizosphere microbiota (Daniel and Bernot, 2014), metabolites (Urano et al., 2010), and related genes. The utilization of multi-omics analysis techniques combining rhizosphere microbiome, metabolome, and transcriptome is an effective method for exploring the mechanisms underlying plant stress alleviation. Wu et al. (2021) successfully applied this approach in studying cucumber response to hydroxybenzoic acid stress. However, there have been no reports on the application of multi-omics analysis techniques to investigate the mechanism by which sulfate mitigates quincloracinduced damage in tobacco leaves. In this study, we found that oxidizing agent K₂S₂O₈ can significantly reduce phytotoxicity symptoms of tobacco induced by quinclorac. To explore the underlying mechanisms, we integrated biochemical methods, rhizosphere microbiota, metabolome, and transcriptome to investigate the effects of persulfate on both quinclorac-contaminated soil and the tobacco plants. This included examining changes in soil characteristics and soil microbial community, and the expression and metabolism of tobacco plant. The results of this study will provide a foundation for the remediation of herbicide residues in soil within rice-tobacco rotation areas.

2 Materials and methods

2.1 Plant materials and treatments

The main tobacco variety CB-1 in the tobacco-growing area of Fujian province was used as experimental material. The pot experiment was conducted from April to June 2024 at the Fujian Key Laboratory of Crop Breeding by Design, situated within the greenhouse of Fujian Agriculture and Forestry University. The greenhouse environment was maintained at a 16-h day temperature of 22 °C and an 8-h night temperature of 18 °C. The experimental design comprised a control group (denoted as CK) without the addition of either $\rm C_{10}H_5Cl_2NO_2$ or $\rm K_2S_2O_8$ to the soil. The treatment groups included soil added with 0.04 mg/kg $\rm C_{10}H_5Cl_2NO_2$ (denoted as C), and soil amended with both 0.04 mg/kg $\rm C_{10}H_5Cl_2NO_2$ and 100 mg/kg $\rm K_2S_2O_8$ (denoted as CY). Each treatment involved five plants, with three biological replicates for a total of 45 pots.

2.2 Sample collection

The samples were collected at 45 days post-treatment. This included soil samples for soil characteristics, rhizospheric soil for microbial community analysis, and tobacco leaves for gene expression and metabolic profiling of the tobacco plants. For the microbial community analysis, soil samples within a range of 1–4 mm around the roots of the three treatment groups were collected, with approximately 100 g per treatment group. Additionally, 100 g of soil was collected from five pots per treatment group for soil characteristics analysis. For gene expression and metabolic profiling of tobacco, leaves in the 2nd–3rd positions from the top (counting from the uppermost leaf) were selected for this study. A total of ten leaves, sourced from five different plants, were collected as a sample. All samples were collected with three biological replicates. Following collection, the soil samples were stored at –20 °C, while the leaf samples were stored at –80 °C until analysis.

2.3 Investigation of soil physical and chemical properties

The collected soil samples were initially purified to remove impurities, and then passed through a 2 mm mesh for homogenization. The air-dried soil samples were subsequently analyzed for their properties and nutrient content. The organic matter was analyzed according to the NY/T1121.6-2006 method; pH was determined using the NY/T1377-2007 method; total nitrogen level was measured following the NY/T53-1987 method; total phosphorus content was assessed based on the NY/T88-1988 method; total potassium concentration was determined according to the NY/T87-1988 method; available nitrogen were evaluated using the method described in LY/T 1228-2015; available phosphorus levels were evaluated using

the NY/T1121.7-2006 method; and available potassium concentration was measured following the NY/T889-2004 method. Soil particle size measurements were carried out according to the NY/T1121.3-2006 method.

2.4 Metagenomic analysis reveals changes in soil microbial communities

The high-throughput metagenomic sequencing technology was used to investigate changes in soil microbial communities under three treatments. Initially, microbial DNA was extracted and purified from soil samples using a bacteria and fungi genomic extraction kit (Omega D3350-02; Solarbio D2300-100T). The resulting DNA fragments were generated through ultrasound treatment, followed by purification, end-repair, 3'-end adenylation, and ligation with sequencing adapters. Subsequently, agarose gel electrophoresis was employed to select appropriately-sized fragments for PCR amplification library construction. Metagenome sequencing was performed on the Illumina Hiseq2500 platform following standard protocols. After data processing and statistical analysis, including low-quality data filtering, output data generation, and quality control statistics, the metagenome assembly was carried out using MEGAHIT software while QUAST software (Tang and Borodovsky, 2014) evaluated the assembly results by removing contig sequences shorter than 300 bp. Additionally, MetaGeneMark software was used for coding region identification and removal of redundant data. Finally, prediction analysis of tobacco rhizosphere microbial community structure and alpha diversity under different treatments was conducted on BMK Cloud.1

2.5 Transcriptomic analysis

RNA-Seq was used for the treatments and their control to investigate the potential mechanism underlying $K_2S_2O_8$ -mediated $C_{10}H_5Cl_2NO_2$ stress mitigation. Total RNA of samples (C, Y, CK) was extracted using the TRIzol reagent (Invitrogen, USA). RNA sequencing (RNA-Seq) and data processing were performed with the Illumina HiSeq platform at Biomarker Technologies Co., LTD. (Beijing, China) according to Cho et al. (2016). The RNA-Seq data have been submitted in the NCBI Sequence Read Archive (SRA) under the accession number PRJNA1221589.

After excluding reads containing adapter, poly-N, and low-quality sequences, the remaining clean reads were aligned to the reference genome in Sol Genomics Network database.² Subsequently, these aligned reads were assembled and quantitatively analyzed using StringTie software to determine the fragments per kilobase of exon per million fragments mapped (FPKM) values. DEGs were identified using a false discovery rate (FDR) \leq 0.01 and |Fold change| \geq 1.5 while calculating FDR and Fold change (FC) for all genes. Additionally, GO and Kyoto Encyclopedia of Genes and Genomes (KEGG) enrichment analyses were performed for the three comparison groups: CK vs. C, CK vs. CY, and C vs. CY.

2.6 Widely targeted metabolomics analysis

The metabolites of leaf samples at 45 days post-treatment (*C*, CY, and CK) were analyzed using widely targeted metabolomics methods. Freeze-dried leaves were homogenized using a mixer mill (MM 400, Retsch, Germany), and the leaf powder was pooled from each biological replicate sample, 100 mg of this powder was extracted overnight at 4 °C with 0.6 mL of 70% aqueous methanol. The extracts were subjected to analysis using ultra-performance liquid chromatography with electrospray ionization coupled to tandem mass spectrometry (UPLC–ESI–MS/MS) at Biomarker Technologies Co., LTD. (Beijing, China).

Metabolic data from each sample were analyzed using hierarchical cluster analysis (HCA), principal component analysis (PCA), and K-means clustering. HCA and PCA analyses were performed using Software R and GraphPad Prism v9.01 (GraphPad Software Inc., La Jolla, CA, USA), respectively. DEMs among samples from different groups were identified based on the following criteria: VIP \geq 1, |Fold change| \geq 1, and p value <0.01. The Venn diagram illustrates the quantitative relationship among different comparison groups. The Kyoto Encyclopedia of Genes and Genomes (KEGG) compound database³ was utilized for annotating the different metabolites which were then mapped onto the KEGG pathway database.⁴ Pathways containing significantly regulated metabolites underwent further analysis through metabolite sets enrichment analysis (MSEA). Significance assessment was conducted by calculating p-values obtained from hypergeometric tests.

2.7 Integrated multi-omics analysis

The Spearman test method (Heinen and Valdesogo, 2020) was employed to conduct correlation analysis among metabolomics, transcriptomics, and microbiota. Results meeting the criteria of a p-value <0.05 and a Spearman correlation coefficient |r| > 0.8 were chosen for constructing a correlation network.

2.8 Quantitative real-time PCR (qRT-PCR) analysis

Total RNA was isolated from plantlets using TRIzol reagent (Invitrogen) according to the manufacturer's protocol. The extracted RNA was then reverse-transcribed into complementary DNA (cDNA), which was used for quantitative real-time PCR (qRT-PCR) analysis with SYBR Premix ExTaq (Takara). The expression of the Actin gene was employed as an internal control. The experiment was conducted with three biological replicates, each comprising three individual plants, and each sample was analyzed in triplicate. The relative gene expression levels were determined using the $2^{-\Delta\Delta Ct}$ method (Livak and Schmittgen, 2001), and the primer sequences used for qRT-PCR are provided in Supplementary Table 1.

¹ www.biocloud.net

² https://solgenomics.net/organism/Nicotiana_attenuata/genome

³ https://www.kegg.jp/kegg/compound/

⁴ https://www.kegg.jp/kegg/pathway.html

3 Results

3.1 Oxidizing agent $K_2S_2O_8$ reduces phytotoxicity symptoms in tobacco induced by $C_{10}H_5Cl_2NO_2$ herbicides

In comparison to the control (CK) (Figure 1A), tobacco seedlings exposed to $C_{10}H_5Cl_2NO_2$ herbicides exhibited leaf curling/narrowing and stunted growth (Figure 1B). Notably, $K_2S_2O_8$ treatment significantly alleviated these symptoms (Figure 1C), suggesting its potential role in mitigating herbicide-induced damage.

3.2 Impacts of $C_{10}H_5Cl_2NO_2$ and $K_2S_2O_8$ on soil physicochemical properties

The physicochemical analysis of the soil (Figure 2) showed $C_{10}H_5Cl_2NO_2$ stress significantly reduced available nitrogen, phosphorus, and potassium (C vs. CK; Figures 2F–H). Importantly, $K_2S_2O_8$ application (CY) counteracted these reductions, restoring available nitrogen and potassium to near-CK levels (Figures 2F,H). Soil particle analysis (Figures 2I–J) further revealed that $C_{10}H_5Cl_2NO_2$ altered granular structure (>0.01 mm vs. <0.01 mm), while $K_2S_2O_8$ rehabilitated proportions to CK-equivalent states. These results demonstrate $K_2S_2O_8$'s dual capacity to alleviate herbicide damage and restore soil functionality.

3.3 Influence of $K_2S_2O_8$ and $C_{10}H_5Cl_2NO_2$ on rhizosphere microbial communities

Metagenomic sequencing of root-associated communities yielded 364,770,378 clean reads from nine samples (treatments C, CY, and the control CK; Supplementary Table 2). Assembly generated 1,133,605 contigs (N50 > 680 bp), with open reading frame (ORF) prediction identifying 2,265,851 ORFs, confirming dataset robustness for further analysis.

Alpha diversity analysis using Shannon, Simpson, and Inverse-Simpson indices demonstrated that $C_{10}H_5Cl_2NO_2$ (C) exposure significantly reduced microbial diversity relative to CK. In contrast, $K_2S_2O_8$ (CY) amendment not only reversed this decline but enhanced

diversity beyond control levels (Figures 3A–C), indicating effective mitigation of herbicide impacts on soil microbiota.

Taxonomic profiling (Supplementary Table 3) identified 4 kingdoms, 185 phyla, 305 classes, 495 orders, 928 families, 2,818 genera, and 12,641 species. Bacteria dominated microbial communities (96.05–97.99% relative abundance), with archaea constituting the remainder (Figure 3D). Five core bacterial phyla-Proteobacteria, Acidobacteria, Actinobacteria, Chloroflexi, and Gemmatimonadetes-collectively represented 83.42–87.29% of relative abundance across treatments (Figure 3E). Notably, C₁₀H₅Cl₂NO₂ reduced the abundance of beneficial genera including *Acidobacteria*, *Chloroflexi*, *Gemmatimonadetes*, *Bradyrhizobium*, *Actinobacteria*, *Verrucomicrobia*, *Candidatus-Rokubacteria*, and *Sphingomonas*, while K₂S₂O₈ treatment uniquely restored their prevalence (Figure 3F). These genus-specific shifts substantiate K₂S₂O₈'s capacity to rehabilitate functional soil microbiomes compromised by quinclorac stress.

3.4 Influence of $K_2S_2O_8$ and $C_{10}H_5Cl_2NO_2$ on gene expression profile and metabolites in tobacco leaves

To elucidate the mechanism by which K₂S₂O₈ alleviates C₁₀H₅Cl₂NO₂ stress, we integrated transcriptomic and metabolomic analyses of tobacco leaves under CK, C, and CY treatments. PCA distinguished the C group from CK and CY (Figure 4A). Notably, C₁₀H₅Cl₂NO₂ stress (C vs. CK) induced 3,019 down-regulated and 2,146 up-regulated genes, while K₂S₂O₈ supplementation (CY vs., C) reversed this trend, up-regulating 851 genes and down-regulating 627 genes (Figure 4B). Crucially, 71 DEGs were common across all comparisons (CK vs. C, CK vs. CY, C vs. CY; Figure 4C). Go enrichment confirmed that DEGs were primarily associated with stress response pathways, including cellular process (GO:0009987), metabolic process (GO:0008152), biological regulation (GO:0065007), localization (GO:0051179), response to stimulus (GO:0050896), signaling (GO:0023052). Critically, C₁₀H₅Cl₂NO₂ suppressed expression in these pathways (down-regulated > up-regulated in CK vs. C), while K₂S₂O₈ restored expression levels, directly supporting its role in mitigating phytotoxicity (Figure 4D).

Metabolite profiling revealed distinct clustering among CK, C, and CY groups (Figures 5A–C), validating data robustness. We identified 1,396 metabolites, dominated by terpenoids (17.9%),

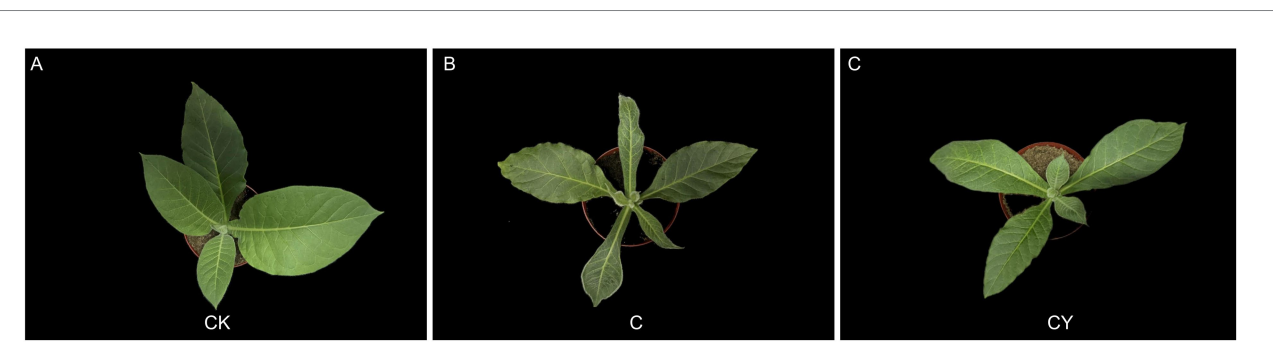
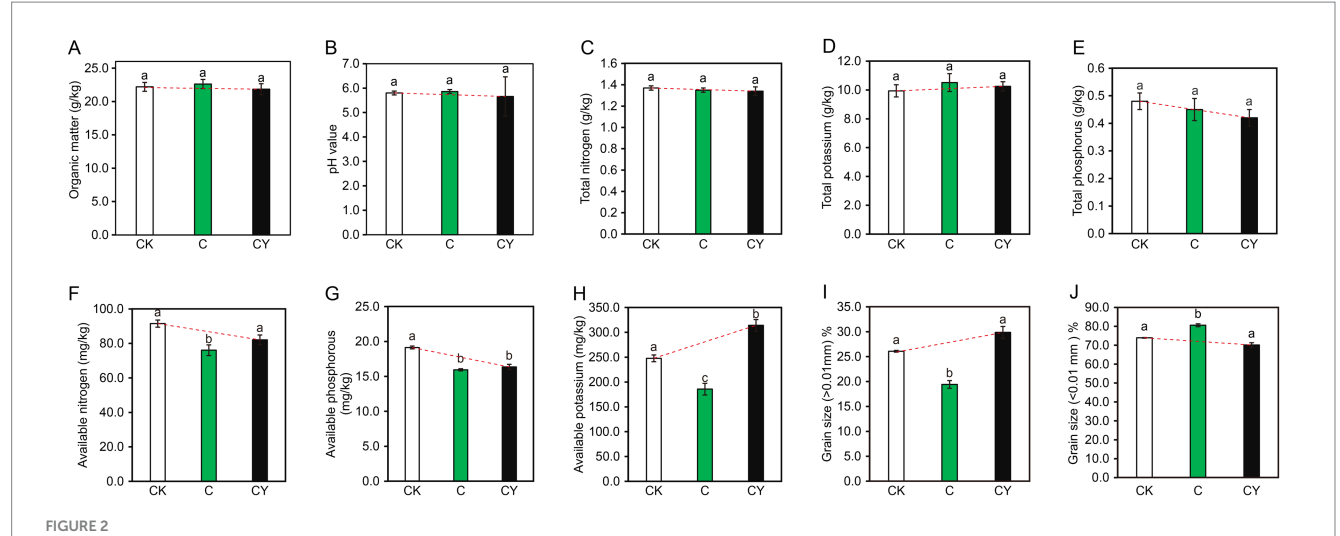
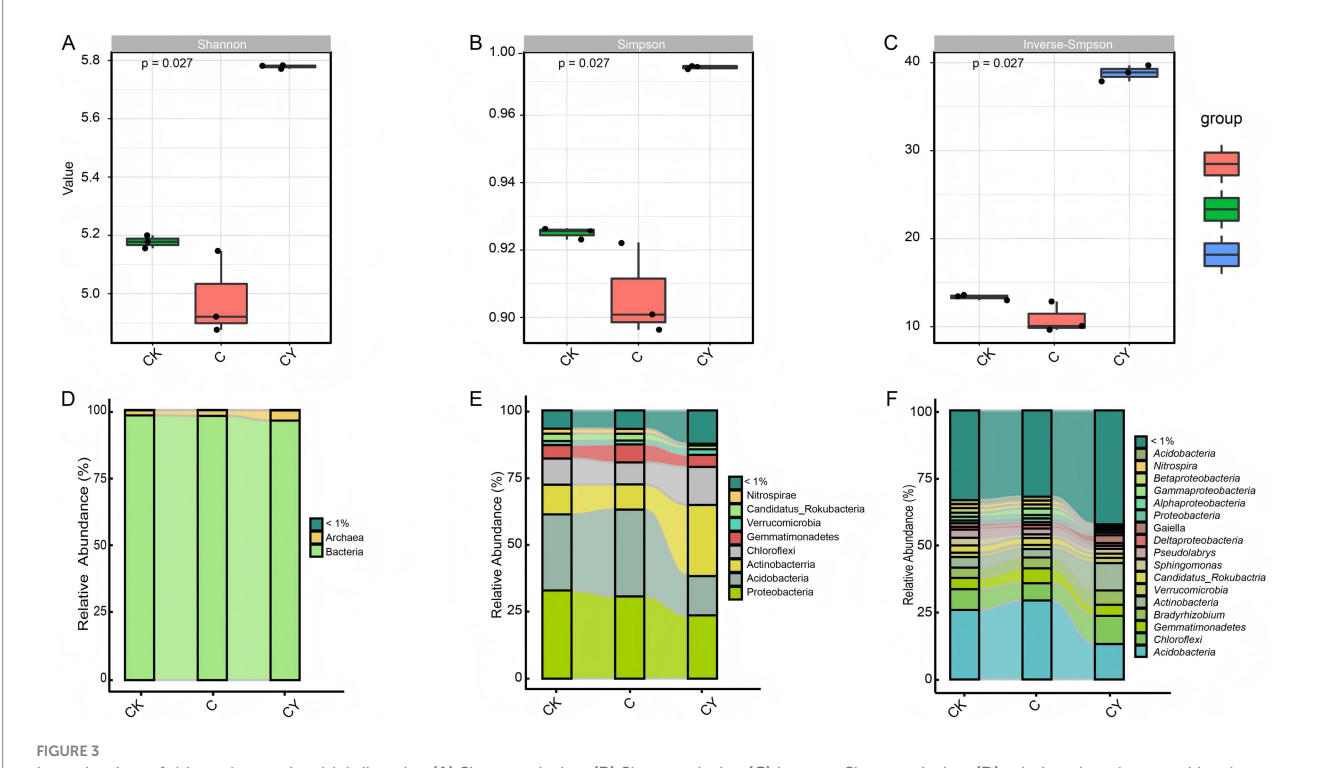


FIGURE 1
The morphology of tobacco leaves under three treatment. (A) Control soil without the addition of C₁₀H₅Cl₂NO₂ or K₂S₂O₈. (B) The soil was treated with 0.04 mg/kg C₁₀H₅Cl₂NO₂. (C) The soil was treated with 0.04 mg/kg C₁₀H₅Cl₂NO₂ and 100 mg/kg K₂S₂O₈.



Impacts of various treatments on soil physicochemical properties. (A) Organic matter, (B) pH value, (C) total nitrogen, (D) total potassium, (E) total phosphorus, (F) available nitrogen, (G) available phosphorus, (H) available potassium, (I) grain size greater than 0.01 mm percentage, (J) grain size less than 0.01 mm percentage. Different lowercase letters after the same column data indicate significant differences among treatments (p < 0.05).

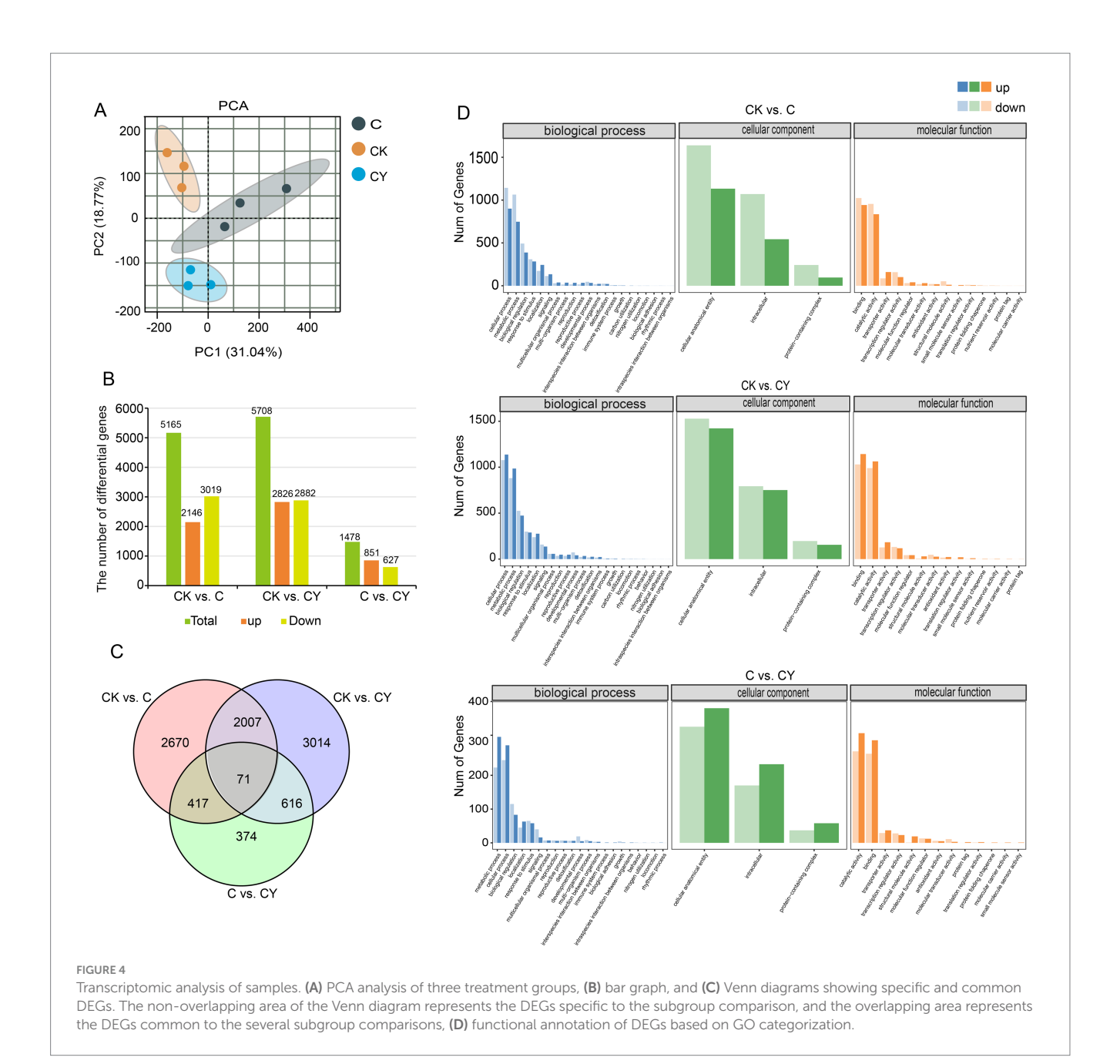


Investigation of rhizosphere microbial diversity. (A) Shannon index, (B) Simpson index (C) Inverse-Simpson index, (D) relative abundance at kingdom level, (E) relative abundance at phylum level, (F) relative abundance at genus level. The different substance categories are represented by different colors in the graph, showing substances that account for more than 1% of the total within each sample group, while the rest are categorized as <1%. The curves illustrate variations in reactant content among different samples.

lipids (11.6%), organic acids (9.03%), sugars/alcohols (8.88%), and amino acids (8.88%) (Figure 5C).

OPLS-DA confirmed significant inter-group differences (Figures 6A–C), and volcano plots quantified metabolites change: CK vs. C had 62 increased and 71 decreased metabolites, while C vs. CY showed 36 increased and 26 decreased metabolites, indicating K₂S₂O₈'s normalization effect (Figures 6D–F). Among 203 differentially

expressed metabolites (DEMs), seven were shared across all comparisons (Figure 6G). K-means clustering demonstrated that $C_{10}H_5Cl_2NO_2$ stress specifically depleted metabolites in cluster 3 and cluster 4 but elevated those in cluster 2 and cluster 5. Remarkably, $K_2S_2O_8$ supplementation (CY) restored these metabolites to nearcontrol (CK) levels (Figure 6H), highlighting its efficacy in rescuing stress-disrupted metabolic pathways.

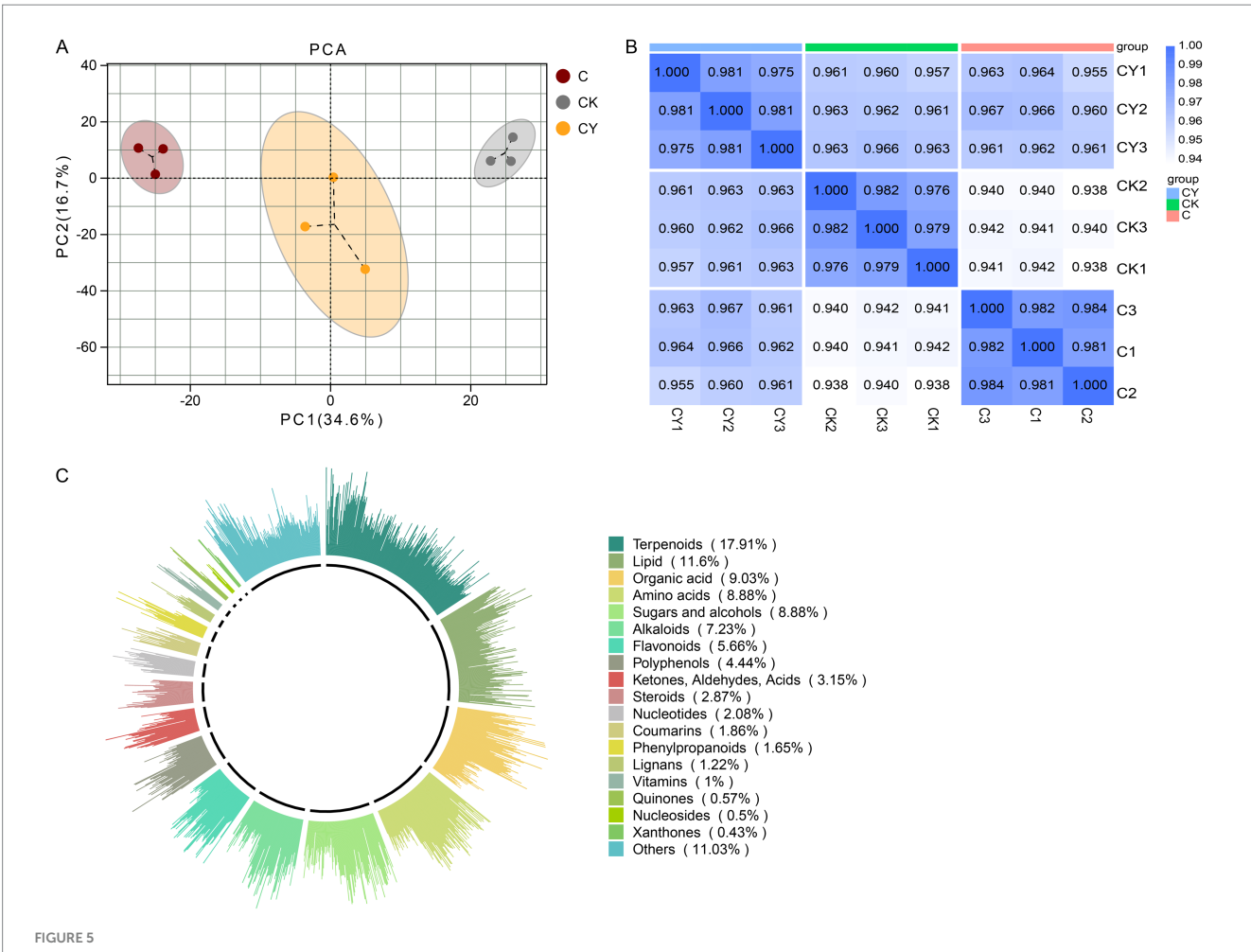


3.5 Integrative analysis of metagenome, transcriptome, and metabolome

To reveal the core metabolic pathways modulated by $K_2S_2O_8$ in alleviating $C_{10}H_5Cl_2NO_2$ stress, we conducted an integrative analysis of metagenome and transcriptome. KEGG analysis identified DEGs and DEMs co-enriched in six key metabolic pathways, including lysine degradation, stilbenoid diarylheptanoid and gingerol biosynthesis, arginine and proline metabolism, phenylalanine biosynthesis, tyrosine metabolism, and flavonoid biosynthesis (Figures 7A–C). A total of 159 DEGs were identified in the six common metabolic pathways, which were classified into 6 clusters by K-means analysis based on their similar expression patterns. Critically, $C_{10}H_5Cl_2NO_2$ stress (C vs. CK) significantly suppressed gene expression in cluster 2 and cluster 4, while inducing expression in cluster 6. Strikingly, $K_2S_2O_8$ supplementation (CY) effectively reversed these stress-induced alterations, restoring

expression levels in these clusters close to those observed in the control (CK) (Figure 7D). This restoration pattern strongly supports $K_2S_2O_8$'s role in counteracting $C_{10}H_5Cl_2NO_2$ -induced dysregulation within these critical pathways. Additionally, compared to control (CK), genes in cluster 1 showed decreasing expression in both C and CY treatments, while genes in cluster 3 exhibited increasing expression in both treatments, though CY induced more pronounced changes than C alone. Among the seven DEMs identified in these six common metabolic pathways, most displayed significantly altered levels under $C_{10}H_5Cl_2NO_2$ stress (CK vs. C) but were restored towards control levels by $K_2S_2O_8$ supplementation (CK vs. C, CK vs. CY) (Figure 7E).

A multi-omics correlation network highlights $K_2S_2O_8$ -mediated regulatory interactions. To elucidate the interplay among metabolomics, transcriptomics, and microbiota, we constructed a correlation network comprising 7 common DEMs, 159 DEGs, and microbial taxa with relative abundance greater than 1% (Figure 7F). The network consists of



Analysis of the metabolite profiles of tobacco in three treatment groups. (A) Score scatter plot for principal component analysis (PCA) model. (B) Analysis of inter-sample correlations. (C) Classification of metabolites in the three treatment groups. The outermost circle of the figure illustrates various types of substances and their relative content. Each class of substances is represented by a specific color, while the length of each column indicates the proportionate content. In the second circle, the length of each line segment represents the proportion of classified substances within the total number. The longer the line segment, the greater number of substances falling under that classification.

79 nodes and 173 edges (96 positive, 77 negative). This included genemicrobe (50 nodes, 112 edges), gene-metabolite (18 nodes, 22 edges), and microbe-metabolite (2 nodes, 3 edges) interactions. Notably, a significant negative correlation was identified between the metabolite 5-Aminovaleric Acid and the microbe Sphingomonas regulated by seven genes (NewGene_3900, Nitab4.5_0000215g0020, Nitab4.5_0000791g0070, Nitab4.5_0000006g0050, Nitab4.5_0001220g0050, Nitab4.5_0000107g0090, and NewGene_21840). Furthermore, 4-Hydroxyphenyacetylgultamic Acid exhibited a significant negative correlation with Bradyrhizobium and Alphaproteobacteria regulated by Nitab_4.50002015 g00700 and Nitab450006992g00700, respectively. These specific regulatory axes underscore the complex interplay between the microbiome, gene expression, and metabolite levels potentially modulated by K₂S₂O₈ in mitigating stress.

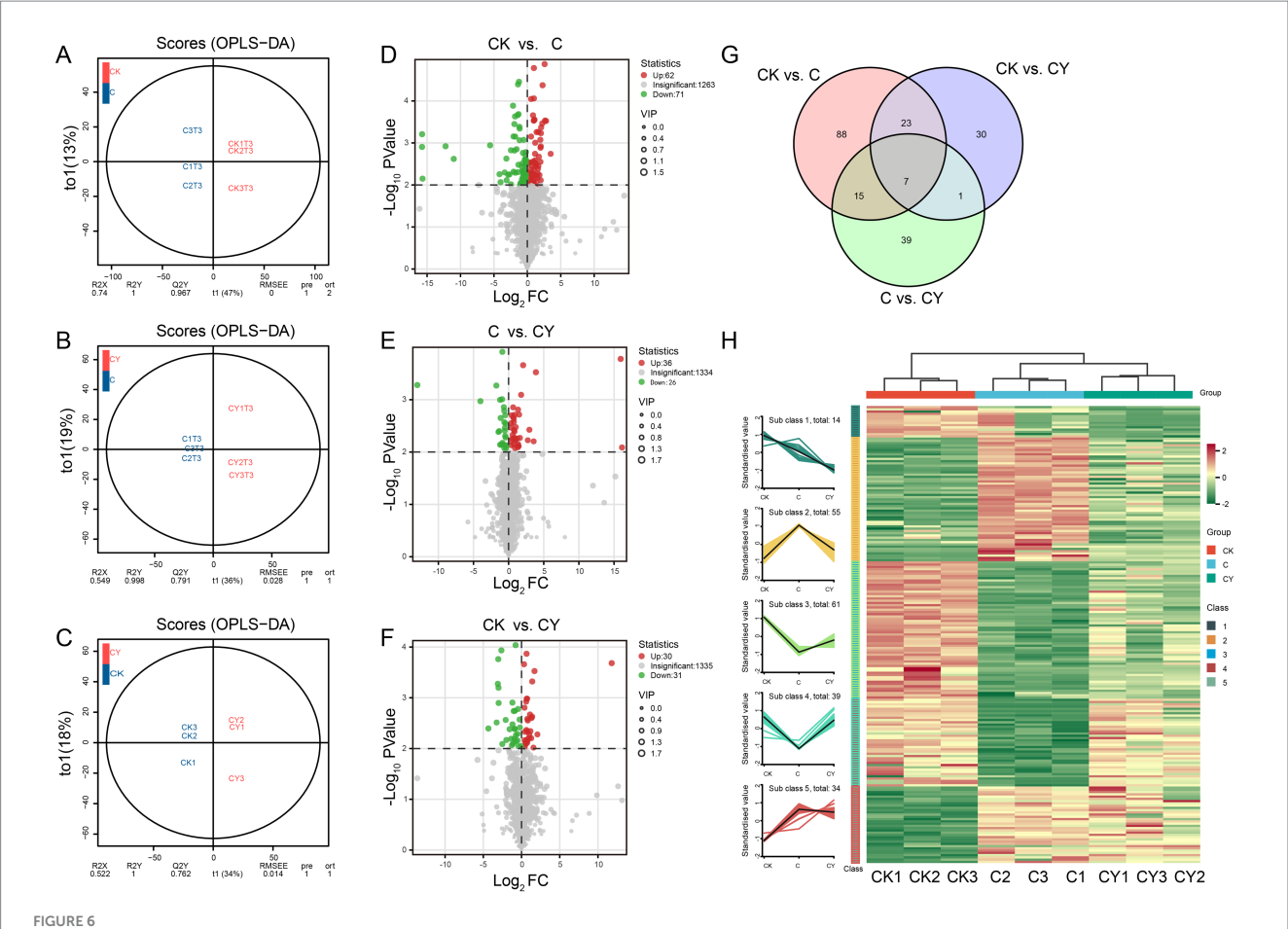
3.6 qRT-PCR validation

To verify the reliability of the transcriptome data, we selected six genes that showed significant correlations with both the metabolome and microbiome for qPCR validation. Compared with the CK group,

the C and CY groups showed consistent trends, with four genes up-regulated and two genes down-regulated. Notably, the gene expression profile of the CY group was more closely aligned with that of the CK group compared to the C group. This observation serves as further evidence of the efficacy of the $K_2S_2O_8$ treatment. The expression patterns of these six genes obtained through qRT-PCR were highly consistent with those from RNA-seq (Figure 8), confirming the reliability of the transcriptome-based differential gene expression analysis.

4 Discussion

Chemical oxidation remediation technology involves the utilization of chemical oxidants to expedite the degradation of pollutants in soil. This technology presents more advantages compared to physical remediation and bioremediation (Dermont et al., 2008), and it has demonstrated extensive application prospects in the field of contaminated site remediation. When compared with conventional oxidants such as Fenton reagent, ozone, and KMnO₄, persulfate-based strategies offer a superior redox potential and a longer half-life in soil

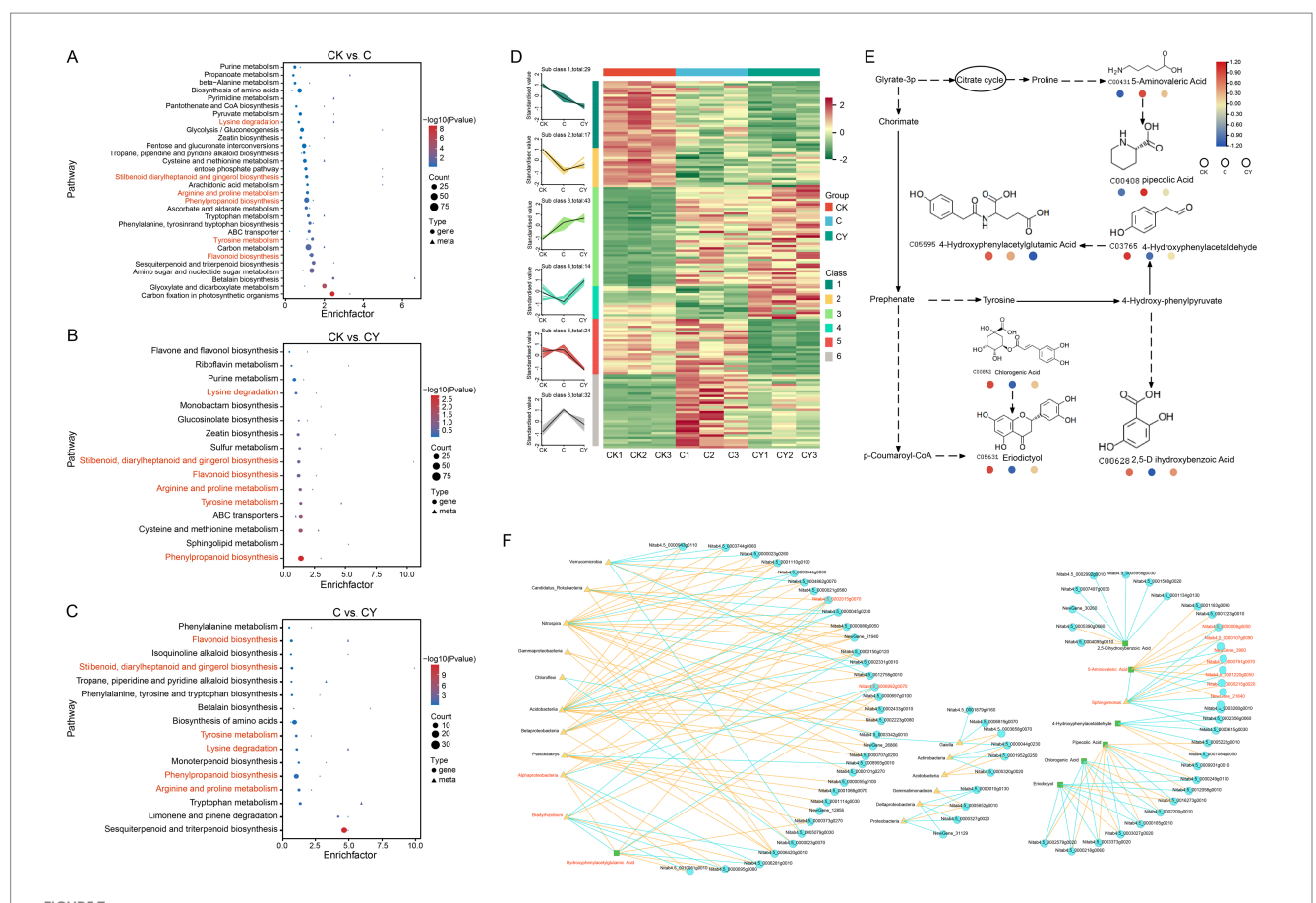


Differential expression metabolites analysis of samples. (A-C) OPLS-DA and (D-F) volcano plot analysis were performed for the comparisons of CK vs. C, C vs. CY, and CK vs. CY. (G) Venn diagram showing the numbers of common and specific DEMs among different comparisons. (H) Line graph and clustered heat-map visualization of significant differentially metabolites based on k-means clustering.

matrices (Yen et al., 2011; Zeng et al., 2016). Previous studies have primarily focused on the degradation of polycyclic aromatic hydrocarbons (PAHs) (Chen et al., 2016) and atrazine (Chen et al., 2018) by persulfate. In this study, we innovatively integrated physiological, biochemical, and multi-omics analysis methods. We comprehensively investigated the effects of potassium persulfate (K₂S₂O₈) on remediating quinclorac-contaminated soil from multiple perspectives, including the impact of the oxidant on plant phenotypes, soil physicochemical properties, and the environmental microecosystem. The results showed that oxidant K2S2O8 can successfully remediate quinclorac-contaminated soil. It not only mitigates quinclorac-induced phytotoxicity, but also replenishes essential soil nutrients (nitrogen, phosphorus, potassium) that are depleted under quinclorac stress (Figure 2). This recovery of soil fertility is vital for sustainable agricultural practices (Daniel and Bernot, 2014), thereby providing new perspectives on addressing a critical challenge in the soil remediation paradigms for rice-tobacco rotation systems.

Secondary metabolic pathways play a crucial role in enabling plants to survive non-biological stress by regulating the levels of secondary metabolites and related gene expression (Lasky et al., 2014). This study integrated transcriptomic and metabolomic analyses to reveal that the DEGs and DEMs identified under quinclorac stress and $K_2S_2O_8$ -mediated stress mitigation were enriched in six metabolic

pathways: diphenyl ethylene diterpenoid biosynthesis, gingerol biosynthesis, arginine and proline metabolism, phenylalanine biosynthesis, tyrosine metabolism, and flavonoid biosynthesis (Figures 7A-C). Of these metabolic pathways, the arginine and proline metabolism directly link with ethylene synthesis through their competition for the common precursor S-adenosylmethionine (SAM), which is essential for both pathways, and through the regulatory interactions that influence the expression of key genes involved in each process (Zhao et al., 2024). All these pathways play a crucial role for regulating secondary metabolites and other protective mechanisms (Arruda and Barreto, 2020; Batista-Silva et al., 2019; Chong et al., 2009; Landi and Gould, 2015; Sharma et al., 2019; Tzin and Galili, 2010). Furthermore, most of the DEGs and DEMs (Figures 7D,E) involved in these pathways exhibited more similar expression levels in the comparison of CK vs. CY treatment compared to CK vs. C, indicating that K₂S₂O₈ application reversed the suppression of these pathways, largely restored the expression of most genes and the levels of key metabolites in these pathways towards those observed in the control. Moreover, it is reported that quinclorac can act as an auxin agonist to activate auxin signaling pathways in plants, leading to growth regulation and inhibition in susceptible species such as tobacco (Song et al., 2022). In this study, we found that at least eight auxin response factor or related genes were up-regulated

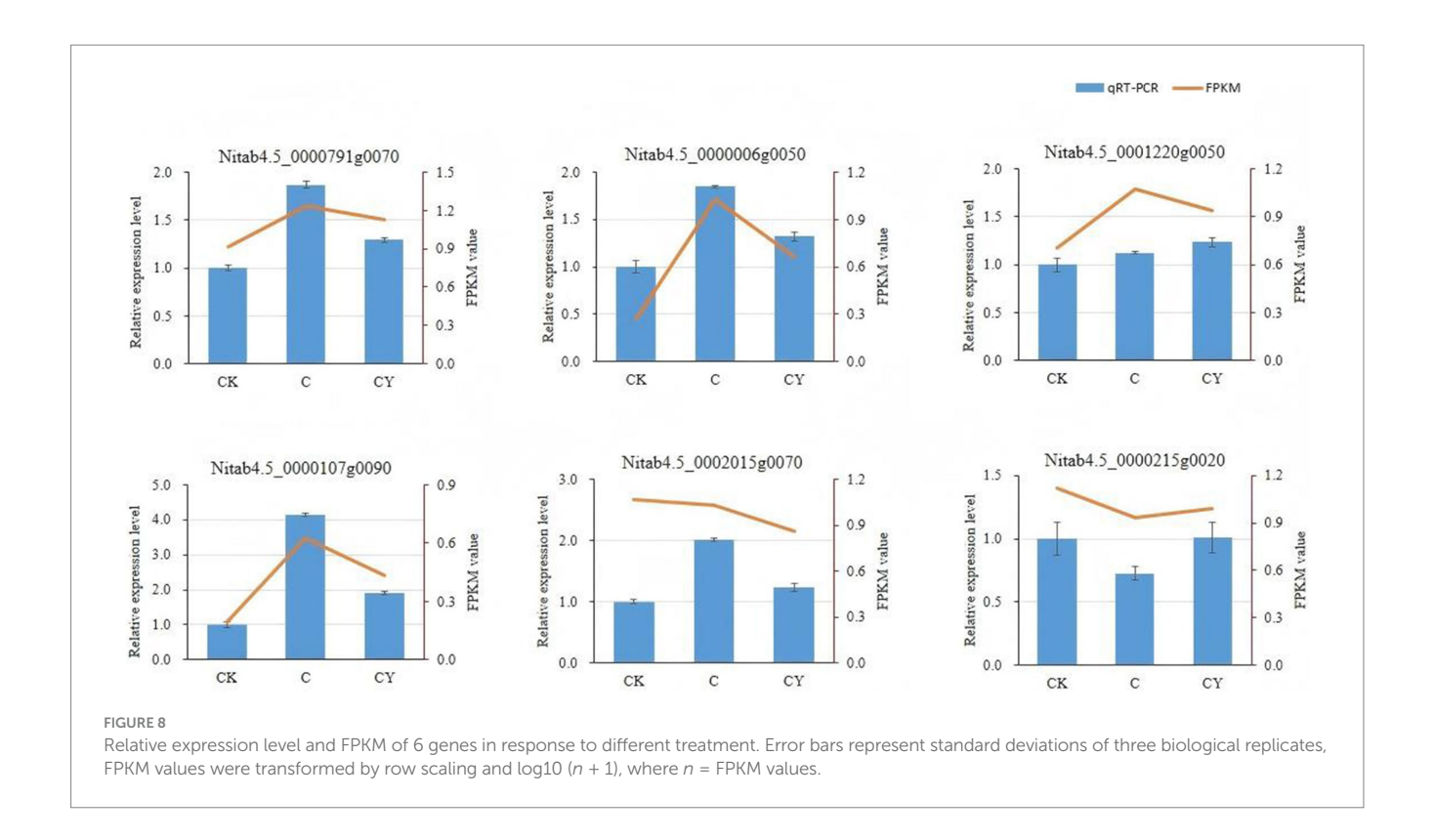


Association analysis of metabolome, transcriptome, and microbiome. (A–C) KEGG enrichment analysis for the DEGs and DEMs in three comparisons: CK vs. C, CK vs. CY, and C vs. CY. The x-axis represents the enrichment factor (Diff/Background) of different omics in this pathway, while the y-axis represents the names of KEGG pathways. The red-blue gradient indicates the degree of enrichment from high to low, as represented by p-value. The shape of bubbles represents different omics, and the size of bubbles represents the number of differential metabolites or genes, with larger bubbles indicating a greater quantity. (D) Line graph and clustered heat-map visualization of 159 significant differentially expressed genes based on k-means clustering. (E) Six shared metabolic pathways in the three comparison groups. (F) The correlation among 7 DEMs, 159 DEGs and the relative abundance (>1%) of microbial taxa at the genus level in three comparison groups. Triangles represent surface microbial genera, circles represent genes, square represent metabolites, and larger triangles, circles or squares indicate higher connectivity among genera, genes, and metabolites. Yellow lines represent positive correlations, while blue lines represent negative correlations.

in CK vs. C group, but down-regulated in C vs. CY treatment, which indicates that $K_2S_2O_8$ treatment reduces the interference of quinclorac on hormone signal transduction.

Quinclorac exposure significantly reduced microbial diversity, disrupting the balance of beneficial taxa such as Acidobacteria, Gemmatimonadetes, Actinobacteria and Chloroflexi. However, K₂S₂O₈ addition remarkably enhanced microbial richness and restored key beneficial genera such as Sphingomonas and Bradyrhizobium (Figure 3). Multi-omics network analysis elucidated the theoretical implications of these microbial shifts, revealing strong correlations between the restored genera (Sphingomonas, Bradyrhizobium), key metabolites (5-aminovaleric 4-hydroxyphenylacetylglutamic acid), and differentially expressed genes (DEGs; e.g., Nitab4.5_0000215g0020, Nitab4.5_0000791g0070) (Figure 7F). These metabolites played a central role in the intricate interplay among soil properties, microbial communities, and plant health—fundamental to agricultural sustainability (Rybnikova et al., 2017). This demonstrates how K₂S₂O₈ reestablishes critical ecological interactions by mitigating quinclorac-induced disruptions to soil structure, nutrient availability, and microbial diversity. The results indicate that $K_2S_2O_8$ fosters a beneficial microbial environment, which crucially modulates plant stress responses through lysine degradation and flavonoid biosynthesis pathways—a novel mechanistic synergy in herbicide remediation. Based on these findings, a hypothetical model was proposed to illustrate the mechanism by which $K_2S_2O_8$ alleviates herbicide damage (Supplementary Figure S1). This enhancement potentially improves nutrient cycling and mitigates phytotoxicity (Sessitsch and Mitter, 2015; Wu et al., 2021), while emphasizing the utility of multi-omics techniques in exploring such complex ecological relationships (Qian et al., 2015; Timmusk and Wagner, 1999). However, more specific mechanistic insights require further in-depth research to fully elucidate the underlying processes.

Quinclorac is an auxinic herbicide widely used to control monocotyledonous weeds, particularly in rice cultivation systems. However, its persistence in acidic soils has raised significant concerns due to its phytotoxicity toward subsequent crops, especially *Solanaceous* species such as tobacco, potato, tomato, and eggplant (Grossmann, 1998; Qiuzan et al., 2018). It is reported to be absorbed by plant roots and transported to shoots, where it induces ethylene and cyanide production, alters plant hormone levels, and causes



oxidative stress, ultimately inhibiting growth in sensitive plants (Song et al., 2022). In this study, we demonstrated that quinclorac exposure led to severe growth inhibition in tobacco seedlings, evident through deformities in leaves and roots. This finding is consistent with previous reports that have highlighted the adverse effects of the herbicide on crop health and yield (Huang et al., 2021). When K₂S₂O₈ was introduced into the soil contaminated with quinclorac, it effectively mitigated these detrimental impacts. The crops in the treated soil were able to resume normal growth patterns, which strongly underscores the potential of K₂S₂O₈ as a promising remediation agent for quinclorac-contaminated soil. This outcome vividly demonstrates the practical feasibility of the method. Notably, when applying this method in field environments, a comprehensive consideration of numerous complex factors is necessary. These factors encompass the soil's pH value, its physical and chemical properties, the soil microecological environment, diverse climatic conditions, and the cost of implementation. To reduce costs, minimize environmental impact, and effectively reduce phytotoxicity of the herbicide, we employed a "hole application" method in our field experiments. Before tobacco transplantation, selectively treated only the planting holes and the adjacent soil of the plants with K₂S₂O₈. This targeted approach not only minimizes resource utilization but also reduces potential negative impacts on the broader environment. The results clearly demonstrated that following the K₂S₂O₈ treatment, the plants showed superior growth, and their root systems were more robustly developed throughout both the seedling and mature stages (Supplementary Figure S2). Undoubtedly, additional in-depth exploration is required to formulate a more comprehensive and optimized utilization method for this treatment. Future field-scale studies should carefully address spatial heterogeneity, the effects of rainfall, and long-term microbiome resilience to further enhance soil remediation strategies. This will allow us to fully realize its potential and maximize its benefits in agricultural practices.

5 Conclusion

This study demonstrates that the oxidizing agent K₂S₂O₈ effectively mitigates the adverse effects of quinclorac herbicide on both agricultural soil and tobacco plants. The integration of biochemical, metagenomic, metabolomic, and transcriptomic analyses demonstrated that K2S2O8 significantly mitigated the quinclorac-induced alterations in gene expression and metabolite profiles, bringing them close to control level. Specifically, K₂S₂O₈ increases the abundance of beneficial microbial flora such as Sphingomonas and Bradyrhizobium, while decreasing harmful bacteria. Additionally, it modulates key metabolic pathways affected by quinclorac, such as arginine and proline metabolism, lysine degradation, and flavonoid biosynthesis. Furthermore, K₂S₂O₈ suppresses the quinclorac-induced increase in auxin response factor and related genes, thereby mitigating its interference with hormone signal transduction. This research offers a comprehensive approach to remediate pesticide-contaminated soils in rice-tobacco rotation systems, supporting sustainable agricultural practices.

Data availability statement

The datasets presented in this study can be found in online repositories. The names of the repository/repositories and

accession number(s) can be found in the article/Supplementary material.

Author contributions

BZ: Writing – original draft. TY: Writing – review & editing. CC: Resources, Writing – review & editing. TL: Writing – review & editing, Data curation. NZ: Writing – review & editing, Data curation. FW: Writing – review & editing, Resources. WC: Resources, Writing – review & editing. ZZ: Writing – review & editing, Resources. ZL: Writing – review & editing, Resources. GG: Writing – review & editing. XL: Writing – review & editing. XX: Writing – review & editing.

Funding

The author(s) declare that financial support was received for the research and/or publication of this article. This research was financially supported by China Tobacco Company [110202201028 (LS-12)], Fujian Tobacco Company (2025350000240080). The funders had no role in the study design, data collection and analysis, decision to publish, or preparation of the manuscript.

Conflict of interest

BZ, GG were employed by Fujian Provincial Tobacco Company. CC, FW, WC were employed by Jianning Branch of Sanming Tobacco Company. ZZ, ZL were employed by Changting Branch of Longyan Tobacco Company.

References

Arruda, P., and Barreto, P. (2020). Lysine catabolism through the saccharopine pathway: enzymes and intermediates involved in plant responses to abiotic and biotic stress. *Front. Plant Sci.* 11:587. doi: 10.3389/fpls.2020.00587

Bains, A., Perez-Garcia, O., Lear, G., Greenwood, D., Swift, S., Middleditch, M., et al. (2019). Induction of microbial oxidative stress as a new strategy to enhance the enzymatic degradation of organic micropollutants in synthetic wastewater. *Environ. Sci. Technol.* 53, 9553–9563. doi: 10.1021/acs.est.9b02219

Batista-Silva, W., Heinemann, B., Rugen, N., Nunes-Nesi, A., Araújo, W. L., and Braun, H. P., And Hildebrandt, T. M. (2019). The role of amino acid metabolism during abiotic stress release. *Plant Cell Environ.* 42, 1630–1644. doi: 10.1111/pce.13518

Chen, L., Hu, X., Yang, Y., Jiang, C., Bian, C., Liu, C., et al. (2018). Degradation of atrazine and structurally related S-triazine herbicides in soils by ferrous-activated persulfate: kinetics, mechanisms and soil-types effects. *Chem. Eng. J.* 351, 523–531. doi: 10.1016/j.cej.2018.06.045

Chen, X., Murugananthan, M., and Zhang, Y. (2016). Degradation of P-nitrophenol by thermally activated persulfate in soil system. *Chem. Eng. J.* 283, 1357–1365. doi: 10.1016/j.cej.2015.08.107

Cho, K., Cho, K. S., Sohn, H. B., Ha, I. J., Hong, S. Y., Lee, H., et al. (2016). Network analysis of the metabolome and transcriptome reveals novel regulation of potato pigmentation. *J. Exp. Bot.* 67, 1519–1533. doi: 10.1093/jxb/erv549

Chong, J., Poutaraud, A., and Hugueney, P. (2009). Metabolism and roles of stilbenes in plants. *Plant Sci.* 177, 143–155. doi: 10.1016/j.plantsci.2009.05.012

Daniel, E., and Bernot, M. (2014). Effects of atrazine, metolachlor, carbaryl and chlorothalonil on benthic microbes and their nutrient dynamics. *PLoS One* 9:e109190. doi: 10.1371/journal.pone.0109190

Dermont, G., Bergeron, M., and Mercier, G., And Richer-Laflèche, M. (2008). Soil washing for metal removal: a review of physical/chemical technologies and field applications. *J. Hazard. Mater.* 152, 1–31, doi: 10.1016/j.jhazmat.2007.10.043

The remaining authors declare that the research was conducted in the absence of any commercial or financial relationships that could be construed as a potential conflict of interest.

Generative AI statement

The authors declare that no Gen AI was used in the creation of this manuscript.

Any alternative text (alt text) provided alongside figures in this article has been generated by Frontiers with the support of artificial intelligence and reasonable efforts have been made to ensure accuracy, including review by the authors wherever possible. If you identify any issues, please contact us.

Publisher's note

All claims expressed in this article are solely those of the authors and do not necessarily represent those of their affiliated organizations, or those of the publisher, the editors and the reviewers. Any product that may be evaluated in this article, or claim that may be made by its manufacturer, is not guaranteed or endorsed by the publisher.

Supplementary material

The Supplementary material for this article can be found online at: https://www.frontiersin.org/articles/10.3389/fmicb.2025.1625585/full#supplementary-material

Grossmann, K. (1998). Quinclorac belongs to a new class of highly selective auxin herbicides. Weed Sci. 46, 707–716. doi: 10.1017/S004317450008975X

He, F., Gao, J., Pierce, E., Strong, P. J., and Wang, H., And Liang, L. (2015). In situ remediation technologies for mercury-contaminated soil. *Environ. Sci. Pollut. Res. Int.* 22, 8124–8147, doi: 10.1007/s11356-015-4316-y

Heinen, A., and Valdesogo, A. (2020). Spearman rank correlation of the bivariate student t and scale mixtures of normal distributions. *J. Multivar. Anal.* 179:104650. doi: 10.1016/j.jmva.2020.104650

Huang, S., Pan, J., Tuwang, M., Li, H., Ma, C., and Chen, M., And Lin, X. (2021). Isolation, screening, and degradation characteristics of a quinclorac-degrading bacterium, strain D, and its potential for bioremediation of rice fields polluted by quinclorac. *Microbiol. Spectr.* 9,:E0039821, doi: 10.1128/Spectrum. 00398-21

Kieling, U., and Pfenning, M. (1990). Quinclorac, a new herbicide for the use in various production systems in seeded rice. Netherlands: Springer Netherlands. doi: 10.1007/978-94-009-0775-1_30

Landi, T., and Gould, A. K. S. (2015). Multiple functional roles of anthocyanins in plant–environment interactions. *Environ. Exp. Bot.* 119, 4–17. doi: 10.1016/j.envexpbot.2015.05.012

Lasky, J. R., Des Marais, D. L., Lowry, D. B., Povolotskaya, I., Mckay, J. K., Richards, J. H., et al. (2014). Natural variation in abiotic stress responsive gene expression and local adaptation to climate in *Arabidopsis Thaliana*. *Mol. Biol. Evol.* 31, 2283–2296. doi: 10.1093/molbev/msu170

Li, L., Wang, Y., Liu, L., Gao, C., Ru, S., and Yang, L. (2024). Occurrence, ecological risk, and advanced removal methods of herbicides in waters: a timely review. *Environ. Sci. Pollut. Res. Int.* 31, 3297–3319. doi: 10.1007/s11356-023-31067-6

Livak, K. J., and Schmittgen, T. D. (2001). Analysis of relative gene expression data using real-time quantitative PCR and the $2^{-\Delta\Delta CT}$ method. *Methods* 25, 402–408. doi: 10.1006/meth.2001.1262

Marcon, L., and Oliveras, J., And Puntes, V. F. (2021). In situ nanoremediation of soils and groundwaters from the nanoparticle's standpoint: a review. *Sci. Total Environ.* 791;:148324, doi: 10.1016/j.scitotenv.2021.148324

- Peng, H., Xu, L., Zhang, W., Liu, F., Lu, X., Lu, W., et al. (2017). Different kinds of persulfate activation with base for the oxidation and mechanism of BDE209 in a spiked soil system. *Sci. Total Environ.* 574, 307–313. doi: 10.1016/j.scitotenv.2016.09.057
- Qian, H., Lu, H., Ding, H., Lavoie, M., Li, Y., and Liu, W., And Fu, Z. (2015). Analyzing *Arabidopsis Thaliana* root proteome provides insights into the molecular bases of enantioselective imazethapyr toxicity. *Sci. Rep.* 5,:11975, doi: 10.1038/srep11975
- Qiuzan, Z., Shuqing, W., and Changyou, S., And Yi, L. (2018). Decay of quinclorac in acidic paddy soil and risk evaluation to the subsequent crop, tobacco (*Nicotiana tabacum* L.). *Bull. Environ. Contam. Toxicol.* 101, 284–287. doi: 10.1007/s00128-018-2372-y
- Rybnikova, V., Singhal, N., and Hanna, K. (2017). Remediation of an aged PCP-contaminated soil by chemical oxidation under flow-through conditions. *Chem. Eng. J.* 314, 202–211. doi: 10.1016/j.cej.2016.12.120
- Sessitsch, A., And Mitter, B. (2015). 21st century agriculture: integration of plant microbiomes for improved crop production and food security. *Microb. Biotechnol.* 8, 32–33, doi: 10.1111/1751-7915.12180
- Sharma, A., Shahzad, B., Rehman, A., Bhardwaj, R., Landi, M., and Zheng, B. (2019). Response of phenylpropanoid pathway and the role of polyphenols in plants under abiotic stress. *Molecules* 24:2452. doi: 10.3390/molecules24132452
- Song, Y., Fang, G., Zhu, C., Zhu, F., Wu, S., Chen, N., et al. (2019). Zero-valent iron activated persulfate remediation of polycyclic aromatic hydrocarbon-contaminated soils: an in situ pilot-scale study. *Chem. Eng. J.* 355, 65–75. doi: 10.1016/j.cej.2018.08.126
- Song, D., Jiang, X., Wang, D., Fang, S., Zhou, H., and Kong, F. (2022). From the effective herbicide to the environmental contaminant: a review of recent studies on quinclorac. *Environ. Exp. Bot.* 193:104706. doi: 10.1016/j.envexpbot.2021.104706
- Sun, J., Pan, L., Tsang, D. C. W., Zhan, Y., and Li, X. (2017). Organic contamination and remediation in the agricultural soils of China: a critical review. *Sci. Total Environ*. 615, 724–740. doi: 10.1016/j.scitoteny.2017.09.271
- Tang, S., And Borodovsky, M. (2014). Ab initio gene identification in metagenomic sequences. New York: Springer New York. doi: 10.1093/nar/gkq275

- Timmusk, S., and Wagner, E. G. (1999). The plant-growth-promoting rhizobacterium *Paenibacillus polymyxa* induces changes in *Arabidopsis thaliana* gene expression: a possible connection between biotic and abiotic stress responses. *Mol. Plant-Microbe Interact.* 12, 951–959. doi: 10.1094/MPMI.1999.12.11.951
- Tzin, V., And Galili, G. (2010). New insights into the shikimate and aromatic amino acids biosynthesis pathways in plants. *Mol. Plant* 3, 956–972, doi: 10.1093/mp/ssq048
- Urano, K., Kurihara, Y., and Seki, M., And Shinozaki, K. (2010). 'Omics' analyses of regulatory networks in plant abiotic stress responses. *Curr. Opin. Plant Biol.* 13, 132–138, doi: 10.1016/j.pbi.2009.12.006
- Wu, F., Ding, Y., Nie, Y., Wang, X. J., An, Y. Q., Roessner, U., et al. (2021). Plant metabolomics integrated with transcriptomics and rhizospheric bacterial community indicates the mitigation effects of *Klebsiella Oxytoca* P620 on P-hydroxybenzoic acid stress in cucumber. *J. Hazard. Mater.* 415:125756. doi: 10.1016/j.jhazmat.2021.125756
- Yen, C. H., Chen, K. F., Kao, C. M., Liang, S. H., and Chen, T. Y. (2011). Application of persulfate to remediate petroleum hydrocarbon-contaminated soil feasibility and comparison with common oxidants. *J. Hazard. Mater.* 186, 2097–2102. doi: 10.1016/j.jhazmat.2010.12.129
- Yu, T., Wang, L., Ma, F., Wang, Y., and Bai, S. (2019). A bio-functions integration microcosm: self-immobilized biochar-pellets combined with two strains of bacteria to remove atrazine in water and mechanisms. *J. Hazard. Mater*:121326. doi: 10.1016/j. ihazmat.2019.121326
- Zang, H., Wang, H., Miao, L., Cheng, Y., Zhang, Y., Liu, Y., et al. (2020). Carboxylesterase, a de-esterification enzyme, catalyzes the degradation of chlorimuronethyl in *Rhodococcus Erythropolis* D310-1. *J. Hazard. Mater.* 387:121684. doi: 10.1016/j.jhazmat.2019.121684
- Zeng, G., Huang, D., Lai, C., Xu, P., Zhang, C., and Liu, Y. (2016). Hydroxyl radicals based advanced oxidation processes (AOPs) for remediation of soils contaminated with organic compounds: a review. *Chem. Eng. J.* 284, 582–598. doi: 10.1016/j.cej.2015.09.001
- Zhao, X., Wang, S., and Guo, F., And Xia, P. (2024). Genome-wide identification of polyamine metabolism and ethylene synthesis genes in *Chenopodium Quinoa* Willd. And their responses to low-temperature stress. *BMC Genomics* 25:370, doi: 10.1186/s12864-024-10265-7